Supporting Information

Lanthanide Chains containing Naphthalenyl Nitronyl Nitroxide Radical

Charlie V. Sarmiento[a], Thamyres A. Araujo[b], Samira G. Reis[b], Mateus S. de Souza,[b] Rafael A. Allão Cassaro,[c]* Miguel A. Novak,[a] Maria G.F. Vaz[b]*

[a] Instituto de Física, Universidade Federal do Rio de Janeiro, Rio de Janeiro, RJ, Brasil

[b] Instituto de Química, Universidade Federal de Fluminense, Niterói, RJ, Brasil

[c] Instituto de Química, Universidade Federal do Rio de Janeiro, Rio de Janeiro, RJ, Brasil

Table of contents

Table S1: Summary of data collection and refinement for **1-4**

Identification	(**1**)	(**2**)	(**3**)	(**4**)
Formula	$C_{32}H_{22}F_{18}GdN_2O_8$	$C_{32}H_{22}F_{18}DyN_2O_8$	$C_{32}H_{22}F_{18}TbN_2O_8$	$C_{49}H_{41}F_{18}N_4O_{14}Y$
Fw (g mol^{-1})	1061.76	1067.01	1063.43	1340.77
T (K)	150(2)	150(2)	294(2)	292(2)
λ (Å)	0.71073	0.71073	0.71073	0.71073
Crystal system	Monoclinic	Monoclinic	Monoclinic	Triclinic
Space group	*P2₁/n*	*P2₁/n*	*P2₁/n*	*P-1*
a (Å)	22.2869(17)	22.2970(9)	22.5914(10)	12.7544(8)
b (Å)	16.8565(15)	16.8233(6)	17.0984(6)	14.3568(10)
c (Å)	22.8736(19)	22.8137(8)	22.9681(10)	19.1732(12)
α (Deg,)	90	90	90	73.103(3)
β (Deg,)	114.560(4)	114.398(2)	114.802(2)	88.416(3)
γ(Deg,)	90	90	90	68.899(3)
Volume ($Å^3$)	7815.7(11)	7793.4(5)	8053.7(6)	3122.4(4)
Z	8	8	8	2
ρ_{calc} (Mg m^{-3})	1.805	1.819	1.754	1.426
μ (mm^{-1})	1.833	2.054	1.888	1.047
F(000)	4144	4160	4152	1352
θ range (Deg.)	2.009-25.462	2.060-26.452	2.043-25.349	2.203-23.256
Index ranges	$-26 \le h \le 26$	$-27 \le h \le 27$	$-27 \le h \le 27$	$-14 \le h \le 14$
	$-17 \le k \le 20$	$-21 \le k \le 21$	$-20 \le k \le 20$	$-15 \le k \le 15$
	$-27 \le l \le 26$	$-26 \le l \le 28$	$-27 \le l \le 27$	$-21 \le l \le 21$
Data collected	99215	151546	453485	47995
Independent reflections	14399	15994	14753	8647
R_{int}	0.0681	0.0759	0.1202	0.0772
Data/restraints/parameters	14399 /144 /1119	15994/144/1101	14753 / 48 / 1126	8647 / 72 / 802
GOF on F^2	1.064	1.094	1.207	1.006
R1,wR2 [I>2σ(I)]	0.0731, 0.1559	0.0477, 0.0996	0. 0595, 0.1235	0.1023, 0.2283
R1,wR2 (all)	0.1002, 0.1729	0.0776, 0.11196	0.0871, 0.1410	0.1288, 0.2459
$\Delta\rho_{max}$, $\Delta\rho_{min}$ ($e \cdot Å^{-3}$)	4.209, -3.973	2.369, -1.544	2.544, -1.505	0.951, -0.753

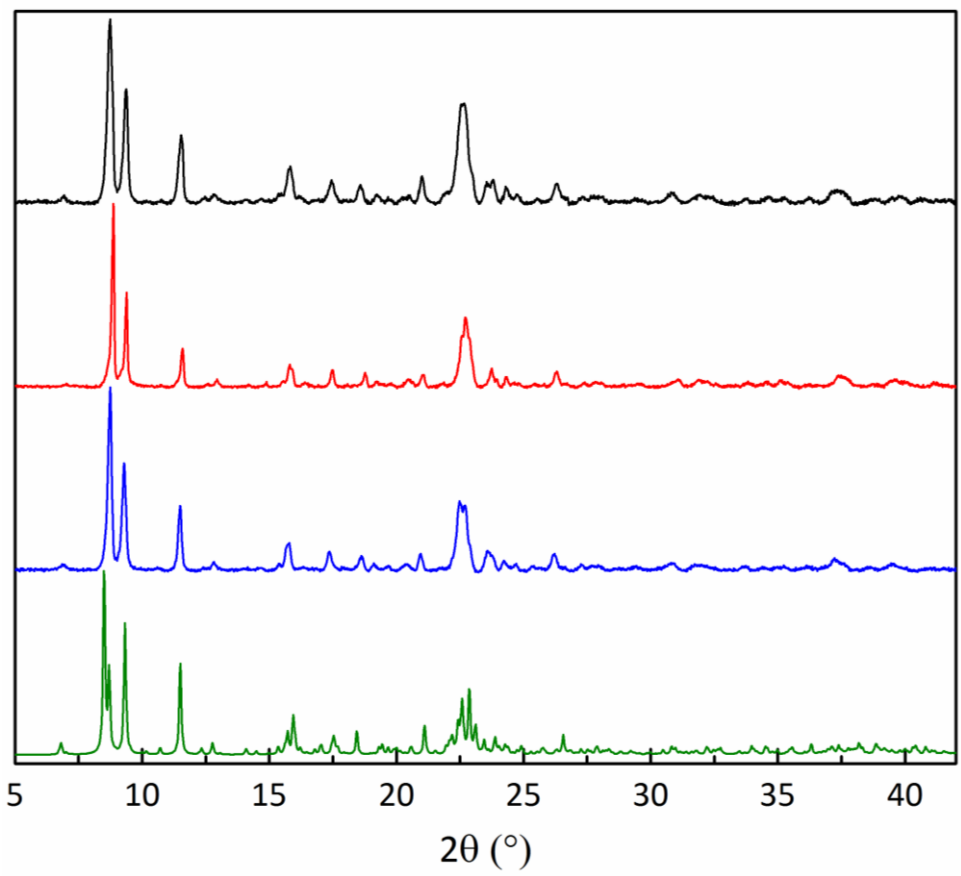

Fig. S1. Powder X-ray diffraction pattern for **1** (blue), **2** (red) and **3** (black) and simulated one (green) from the crystal structure of **2**.

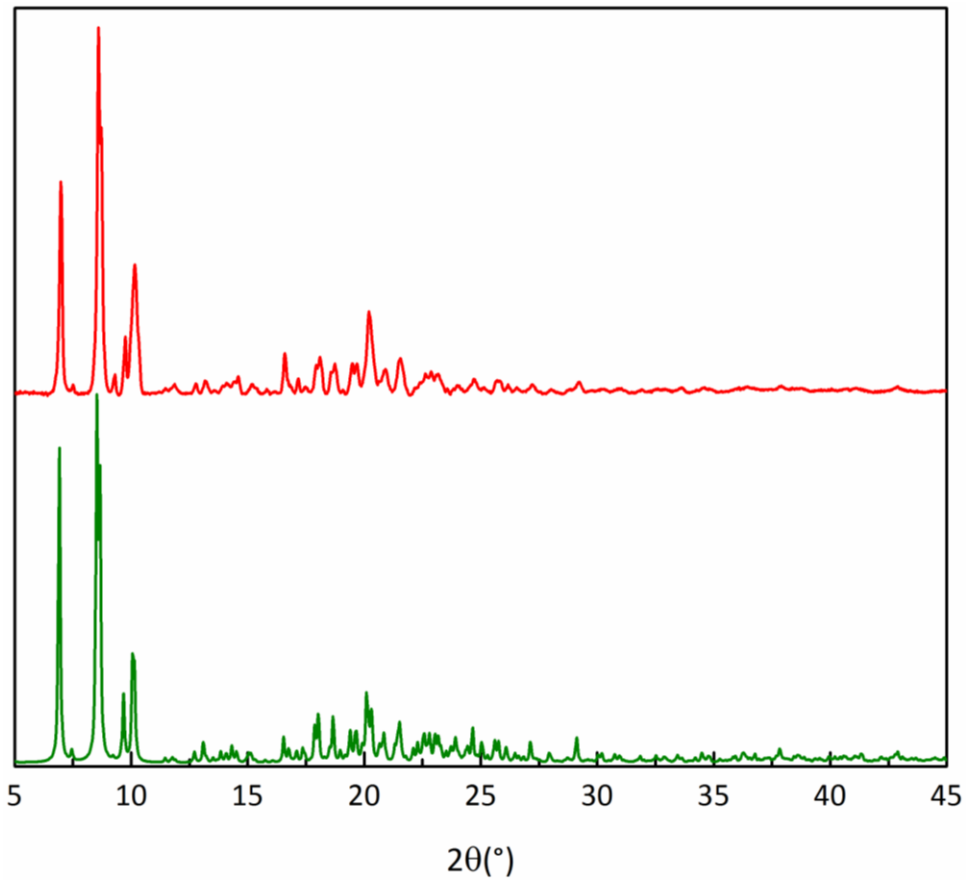

Fig. S2: Powder X-ray diffraction pattern for **4** (red) and simulated one (green) from the crystal structure of **4**.

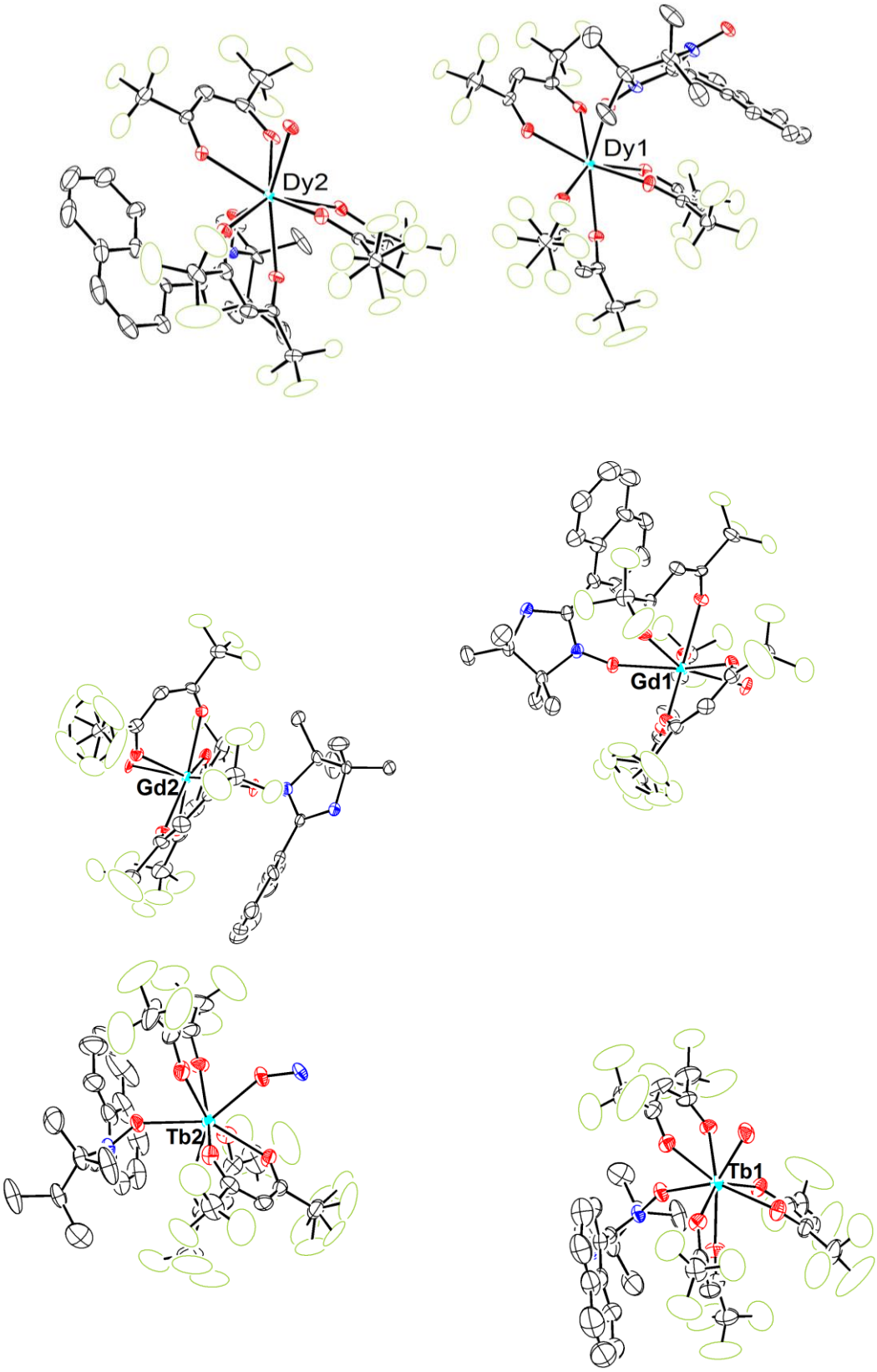

Fig. S3. : ORTEP view of the asymmetric unit of **1-3** at 30% of probability. Color code: black, blue, red, green and cyan stands for carbon, nitrogen, oxygen, fluorine atoms and lanthanide (III) ions, respectively. Hydrogen atoms were omitted for clarity.

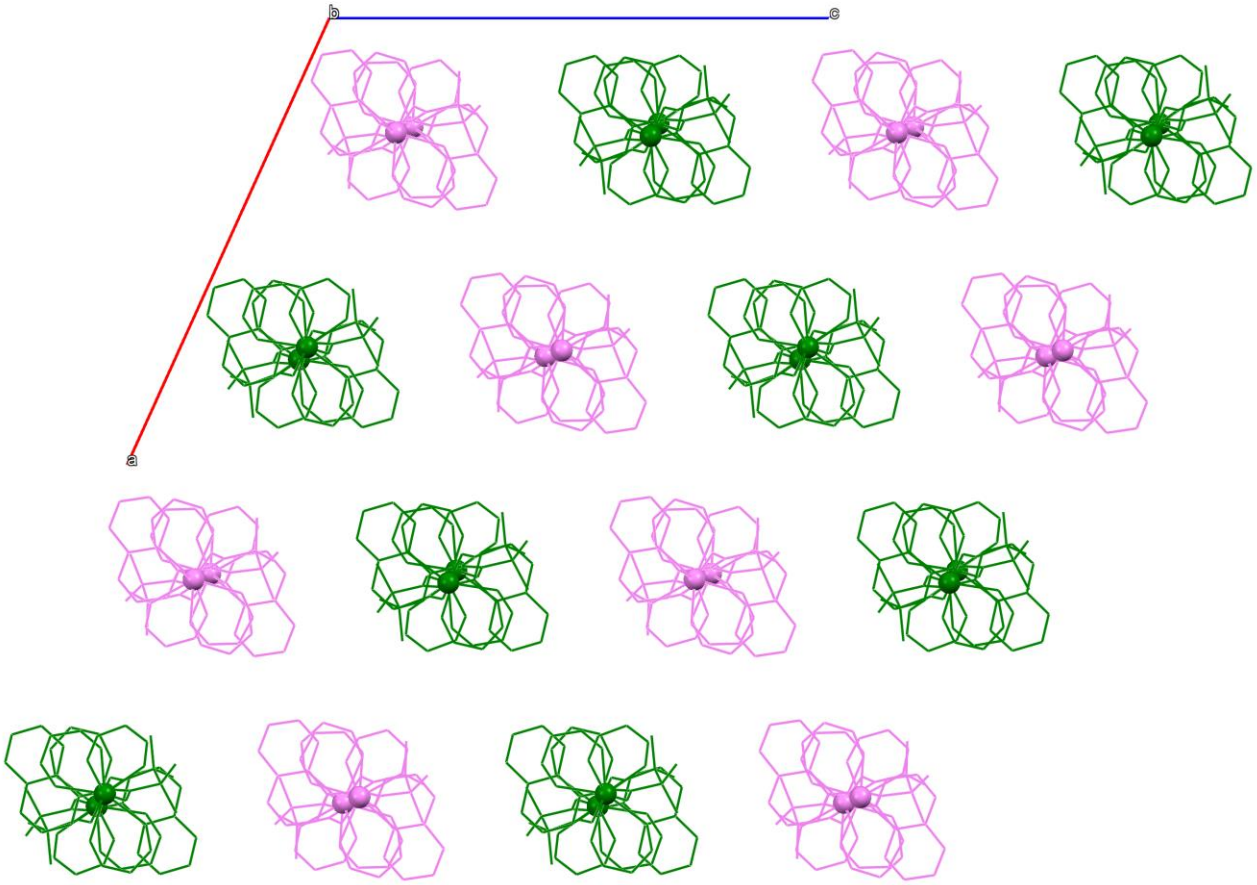

Fig. S4. View of the crystal packing of **1-3** along the crystallographic *b* axis emphasizing the arrangement of the two crystallographically non-equivalent chains containing Ln1 (green) and Ln2 (pink).

Table S2: CSM Calculations of the coordination environment of LnO8 in **1-4**

Ln ion	OP-8	HPY-8	HBPY-8	CU-8	SAPR-8	TDD-8	JGBF-8	JETBPY-8	JBTPR-8	BTPR-8	JSD-8	TT-8	ETBPY-8
Gd1	29.667	23.490	14.401	7.951	1.850	**0.443**	14.546	27.648	2.681	2.091	3.217	8.779	23.028
Gd2	30.524	22.967	13.062	7.957	2.690	**0.612**	13.363	27.372	3.037	2.186	3.583	8.693	22.839
Dy1	29.690	23.762	14.616	7.896	1.801	**0.366**	14.743	28.158	2.665	2.056	3.157	8.725	23.393
Dy2	30.773	23.228	13.251	7.856	2.705	**0.500**	13.741	27.961	2.999	2.168	3.479	8.599	23.141
Tb1	30.248	23.410	14.710	8.130	2.193	**0.279**	14.220	28.555	2.712	2.101	2.969	8.967	23.577
Tb2	30.974	23.284	13.617	8.154	2.750	**0.450**	14.042	28.143	2.970	2.147	3.367	8.893	23.680
Y1	30.387	24.433	15.032	8.042	1.873	**0.192**	14.674	28.891	2.480	2.035	2.665	8.827	24.479

OP-8 Octagon; HPY-8 Heptagonal pyramid; HBPY-8 Hexagonal bipyramid; CU-8 Cube; SAPR-8 Square antiprism; TDD-8 Triangular dodecahedron; JGBF-8 Johnson gyrobifastigium J26; JETBPY-8 Johnson elongated triangular bipyramid J14, JBTPR-8 Biaugmented trigonal prism J50; BTPR-8 Biaugmented trigonal prism; JSD-8 Snub diphenoid J84; TT-8 Triakis tetrahedron; ETBPY-8 Elongated trigonal bipyramid.

Table S3: Selected bond lengths (Å) and bond angles (º) for **1**-**3.**

Bond lengths					
1		**2**		**3**	
Gd1─O1	2.379(6)	Dy1─O1	2.355(4)	Tb1─O1	2.365(5)
Gd1─O2	2.372(6)	Dy1─O2	2.333(4)	Tb1─O2	2.353(5)
Gd1─O3	2.336(6)	Dy1─O3	2.316(4)	Tb1─O3	2.319(5)
Gd1─O4	2.389(7)	Dy1─O4	2.371(4)	Tb1─O4	2.380(6)
Gd1─O5	2.413(6)	Dy1─O5	2.387(4)	Tb1─O5	2.404(6)
Gd1─O6	2.361(7)	Dy1─O6	2.328(4)	Tb1─O6	2.332(5)
Gd1─O7	2.371(7)	Dy1─O7	2.345(4)	Tb1─O7	2.353(6)
Gd1─O8	2.395(7)	Dy1─O8[a]	2.378(4)	Tb1─O8	2.397(6)
Gd2─O9	2.351(7)	Dy2─O9	2.334(4)	Tb2─O9	2.344(6)
Gd2─O10	2.367(7)	Dy2─O10	2.341(4)	Tb2─O10	2.351(6)
Gd2─O11	2.362(7)	Dy2─O11	2.351(4)	Tb2─O11	2.355(5)
Gd2─O12	2.368(7)	Dy2─O12	2.345(4)	Tb2─O12	2.350(5)
Gd2─O13	2.366(7)	Dy2─O13	2.340(4)	Tb2─O13	2.351(6)
Gd2─O14	2.387(7)	Dy2─O14	2.366(4)	Tb2─O14	2.375(6)
Gd2─O15	2.368(6)	Dy2─O15	2.359(4)	Tb2─O15	2.369(5)
Gd2─O16	2.381(7)	Dy2─O16	2.365(4)	Tb2─O16	2.376(5)
Bond angles					
O1─Gd1─O2	72.8(2)	O1─Dy1─O2	73.44(14)	O1─Tb1─O2	72.83(19)
O1─Gd1─O3	70.6(2)	O1─Dy1─O3	70.43(14)	O1─Tb1─O3	71.47(19)
O4─Gd1─O1	125.4(2)	O4─Dy1─O1	125.26(15)	O4─Tb1─O1	127.3(2)
O1─Gd1─O5	127.4(2)	O1─Dy1─O5	127.95(14)	O1─Tb1─O5	127.52(19)
O1─Gd1─O6	152.1(2)	O1─Dy1─O6	151.84(14)	O1─Tb1─O6	150.82(19)
O1─Gd1─O7	70.6(3)	O1─Dy1─O7	71.47(15)	O1─Tb1─O7	71.6(2)
O1─Gd1─O8	80.3(3)	O1─Dy1─O8[a]	78.94(15)	O1─Tb1─O8[a]	79.2(2)
O3─Gd1─O2	143.4(2)	O3─Dy1─O2	143.82(14)	O3─Tb1─O2	144.3(2)
O4─Gd1─O2	134.2(2)	O4─Dy1─O2	133.40(14)	O4─Tb1─O2	133.0(2)
O5─Gd1─O2	129.5(2)	O5─Dy1─O2	129.76(15)	O5─Tb1─O2	130.4(2)
O6─Gd1─O2	79.3(2)	O6─Dy1─O2	78.41(15)	O6─Tb1─O2	78.1(2)
O7─Gd1─O2	74.9(2)	O7─Dy1─O2	75.45(15)	O7─Tb1─O2	75.7(2)
O8─Gd1─O2	68.7(2)	O8[a]─Dy1─O2	69.02(15)	O8[a]─Tb1─O2	69.2(2)
O4─Gd1─O3	71.7(2)	O4─Dy1─O3	72.47(15)	O4─Tb1─O3	72.00(19)
O5─Gd1─O3	74.9(2)	O5─Dy1─O3	74.38(15)	O5─Tb1─O3	74.4(2)
O6─Gd1─O3	137.3(2)	O6─Dy1─O3	137.73(15)	O6─Tb1─O3	137.6(2)
O3─Gd1─O7	91.8(2)	O3─Dy1─O7	91.30(15)	O3─Tb1─O7	93.2(2)
O8─Gd1─O3	105.8(3)	O8[a]─Dy1─O3	105.20(16)	O8[a]─Tb1─O3	103.9(2)
O4─Gd1─O5	76.5(3)	O4─Dy1─O5	76.07(15)	O4─Tb1─O5	75.2(2)
O4─Gd1─O6	75.5(2)	O4─Dy1─O6	74.99(14)	O4─Tb1─O6	75.6(2)
O4─Gd1─O7	147.5(2)	O4─Dy1─O7	147.36(15)	O4─Tb1─O7	146.5(2)
O4─Gd1─O8	73.7(3)	O4─Dy1─O8[a]	73.64(15)	O4─Tb1─O8[a]	73.6(2)
O6─Gd1─O5	71.5(2)	O6─Dy1─O5	72.16(14)	O6─Tb1─O5	71.4(2)
O5─Gd1─O7	72.2(3)	O5─Dy1─O7	72.29(15)	O5─Tb1─O7	71.8(2)
O8─Gd1─O5	148.1(3)	O8[a]─Dy1─O5	148.14(16)	O8[a]─Tb1─O5	147.5(2)
O6─Gd1─O7	102.0(2)	O6─Dy1─O7	102.26(15)	O6─Tb1─O7	99.2(2)
O6─Gd1─O8	90.0(3)	O6─Dy1─O8[a]	90.50(15)	O6─Tb1─O8[a]	92.1(2)
O8─Gd1─O7	138.7(3)	O8[a]─Dy1─O7	138.85(16)	O8[a]─Tb1─O7	139.9(2)
O10─Gd2─O9	72.9(3)	O10─Dy2─O9	73.48(15)	O10─Tb2─O9	73.3(3)
O11─Gd2─O9	130.9(2)	O11─Dy2─O9	130.61(15)	O11─Tb2─O9	131.5(2)
O9─Gd2─O12	80.8(3)	O9─Dy2─O12	79.47(15)	O9─Tb2─O12	79.3(2)
O9─Gd2─O13	143.1(3)	O9─Dy2─O13	143.76(16)	O9─Tb2─O13	143.4

O14─Gd2─O9	134.2(2)	O14─Dy2─O9	133.45(2)	O14─Tb2─O9	133.7(2)
O9─Gd2─O15	68.1(2)	O9─Dy2─O15	68.32(14)	O9─Tb2─O15	69.0(2)
O9─Gd2─O16	72.2(2)	O9─Dy2─O16	72.00(14)	O9─Tb2─O16	72.9
O10─Gd2─O11	122.7(2)	O10─Dy2─O11	123.28(14)	O10─Tb2─O11	123.8(2)
O10─Gd2─O12	153.5(2)	O10─Dy2─O12	152.75(15)	O10─Tb2─O12	152.2(2)
O10─Gd2─O13	70.2(2)	O10─Dy2─O13	70.28(15)	O10─Tb2─O13	70.1(2)
O10─Gd2─O14	126.9(2)	O10─Dy2─O14	127.41(13)	O10─Tb2─O14	127.3(2)
O10─Gd2─O15	84.8(3)	O10─Dy2─O15	83.66(15)	O10─Tb2─O15	83.8(2)
O10─Gd2─O16	72.5(2)	O10─Dy2─O16	73.02(15)	O10─Tb2─O16	72.9(2)
O11─Gd2─O12	72.9(2)	O11─Dy2─O12	73.10(14)	O11─Tb2─O12	73.62(19)
O11─Gd2─O13	72.8(2)	O11─Dy2─O13	72.89(14)	O11─Tb2─O13	73.1(2)
O14─Gd2─O11	77.3(2)	O14─Dy2─O11	76.95(14)	O14─Tb2─O11	76.0(2)
O11─Gd2─O15	148.4(2)	O11─Dy2─O15	148.61(15)	O11─Tb2─O15	147.3(2)
O11─Gd2─O16	70.6(2)	O11─Dy2─O16	70.88(15)	O11─Tb2─O16	71.2(2)
O13─Gd2─O12	136.0(2)	O13─Dy2─O12	136.73(15)	O13─Tb2─O12	137.3(2)
O14─Gd2─O12	74.9(2)	O14─Dy2─O12	74.76(14)	O14─Tb2─O12	75.8(2)
O15─Gd2─O12	88.7(2)	O15─Dy2─O12	89.47(14)	O15─Tb2─O12	90.5(2)
O16─Gd2─O12	96.4(2)	O16─Dy2─O12	95.73(14)	O16─Tb2─O12	95.2(2)
O14─Gd2─O13	71.4(2)	O14─Dy2─O13	72.15(14)	O14─Tb2─O13	71.8(2)
O13─Gd2─O15	107.2(3)	O13─Dy2─O15	106.58(15)	O13─Tb2─O15	105.4(2)
O13─Gd2─O16	97.3(3)	O13─Dy2─O16	97.62(15)	O13─Tb2─O16	97.2(2)
O14─Gd2─O15	73.1(3)	O14─Dy2─O15	73.30(14)	O14─Tb2─O15	72.7(2)
O14─Gd2─O16	147.8(2)	O14─Dy2─O16	147.83(15)	O14─Tb2─O16	147.2(2)
O15─Gd2─O16	138.5(2)	O15─Dy2─O16	138.25(15)	O15─Tb2─O16	139.7(2)

[a] = symmetry operation -x+1/2, y+1/2, -z+3/2

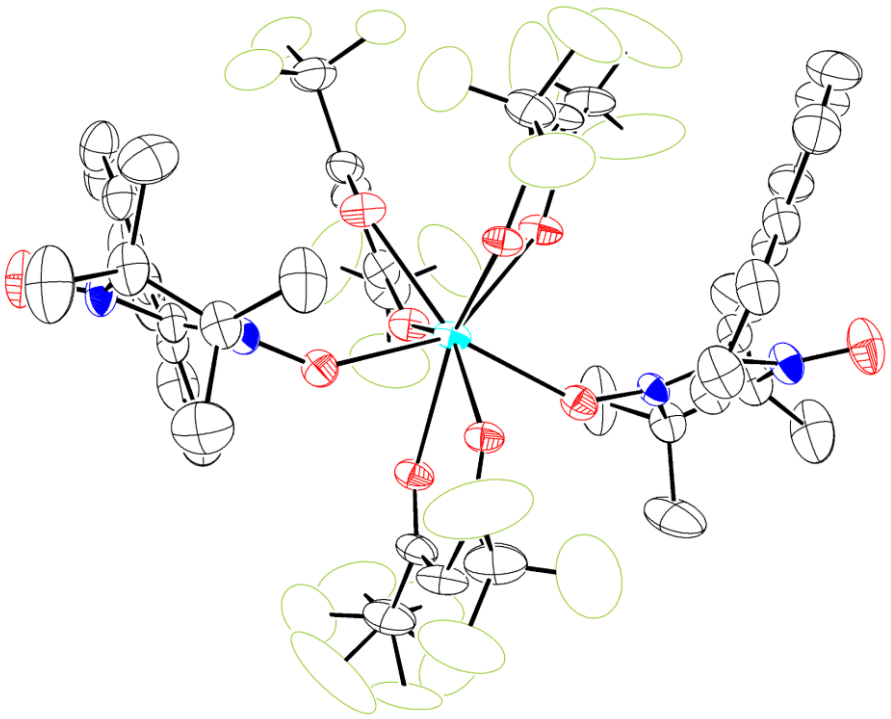

Fig. S5. : ORTEP view of the asymmetric unit of **4** at 30% of probability. Color code: black, blue, red, green and cyan stands for carbon, nitrogen, oxygen, fluorine atoms and yttrium (III) ion, respectively. Hydrogen atoms and oxygen atoms from water molecules were omitted for clarity.

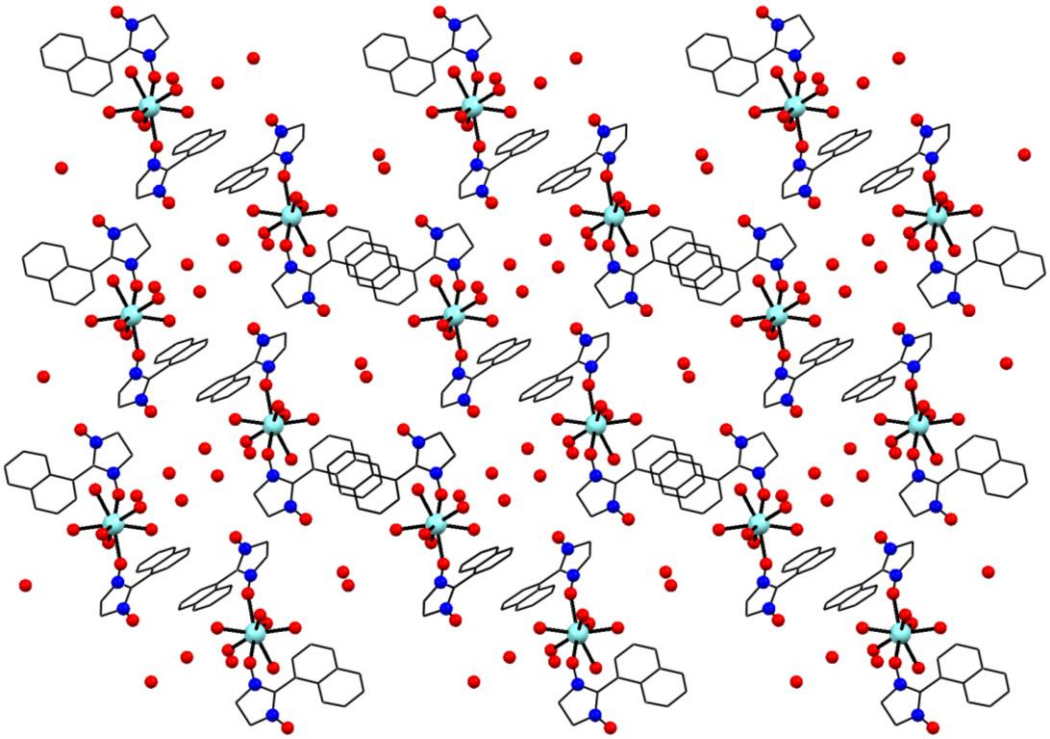

Fig. S6: View of the crystal packing of **4** along the crystallographic *b* axis. Hydrogen atoms, methyl and CF_3 groups were omitted for clarity.

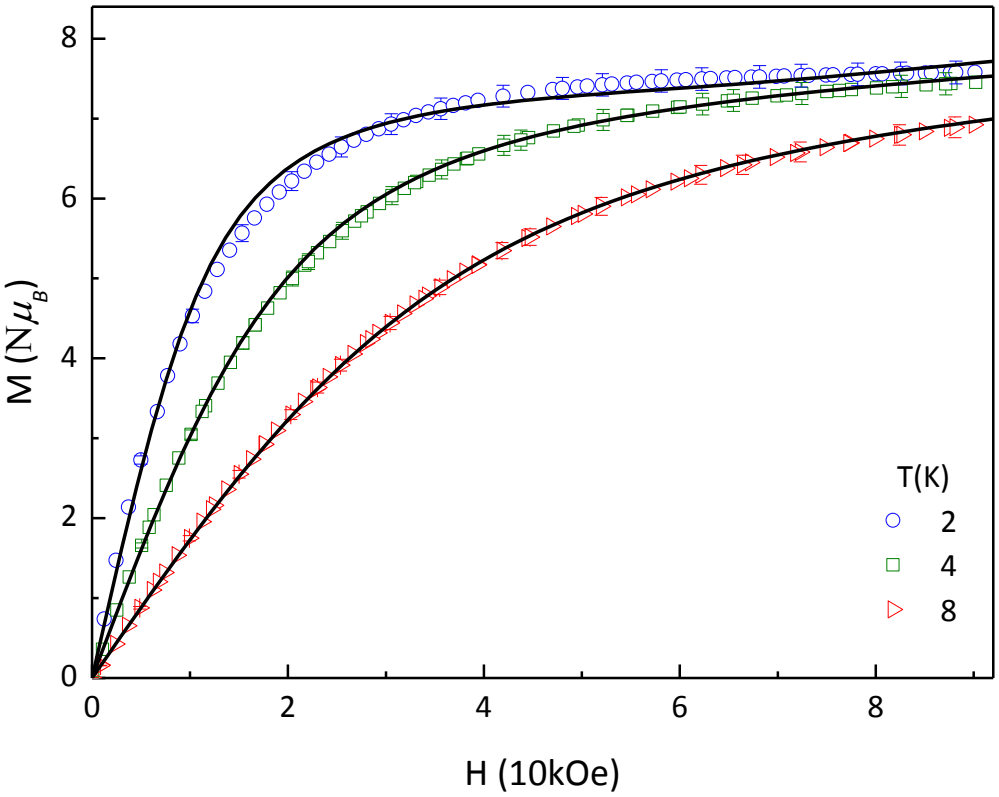

Fig. S7. : Field dependence of magnetization for **1** at different temperatures. The error bar is shown in the Figure. Solid lines represent the best fit using parameters described in the main text.

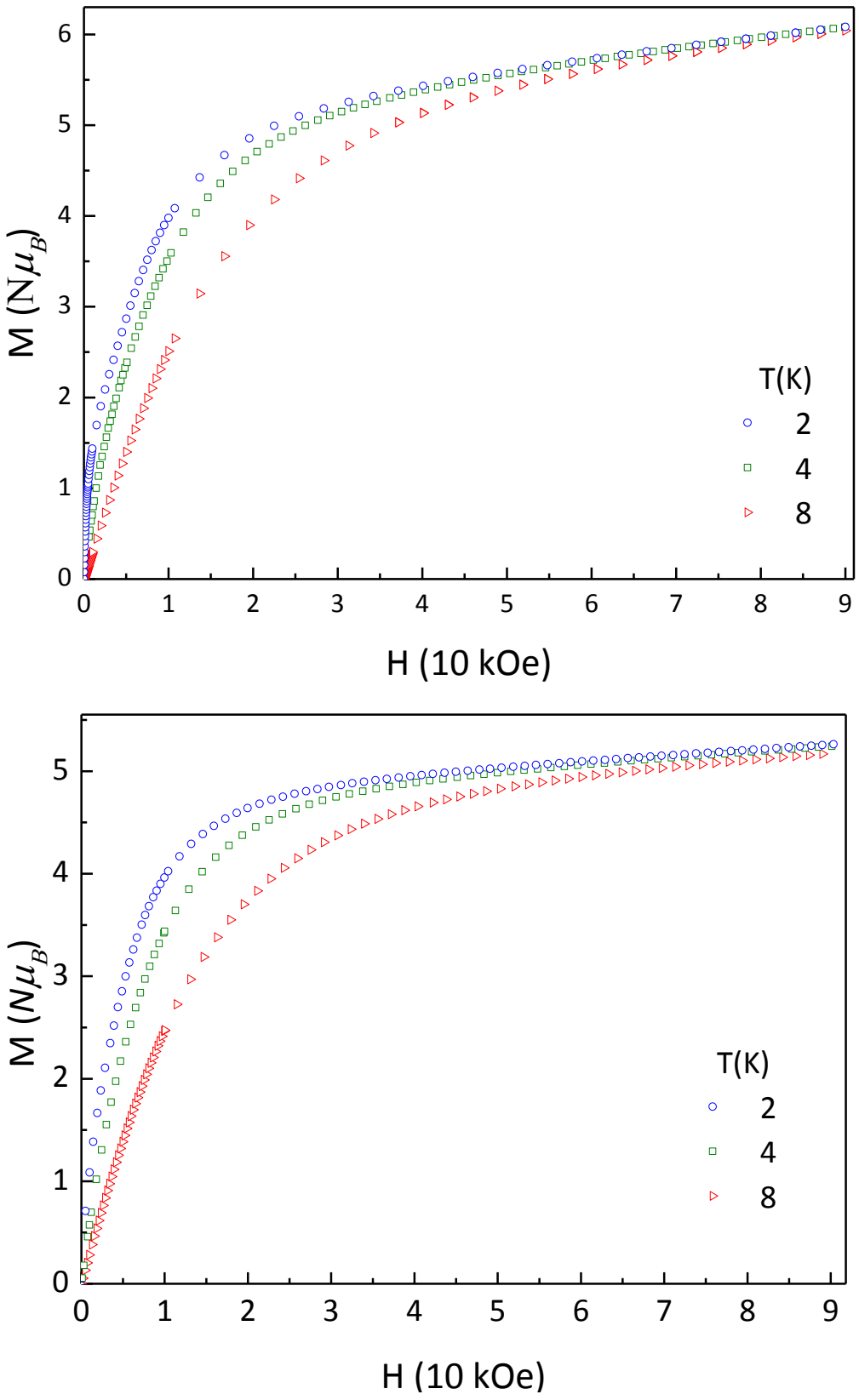

Fig. S8. : Field dependence of magnetization for **2** (top) and **3** (bottom) at different temperatures.

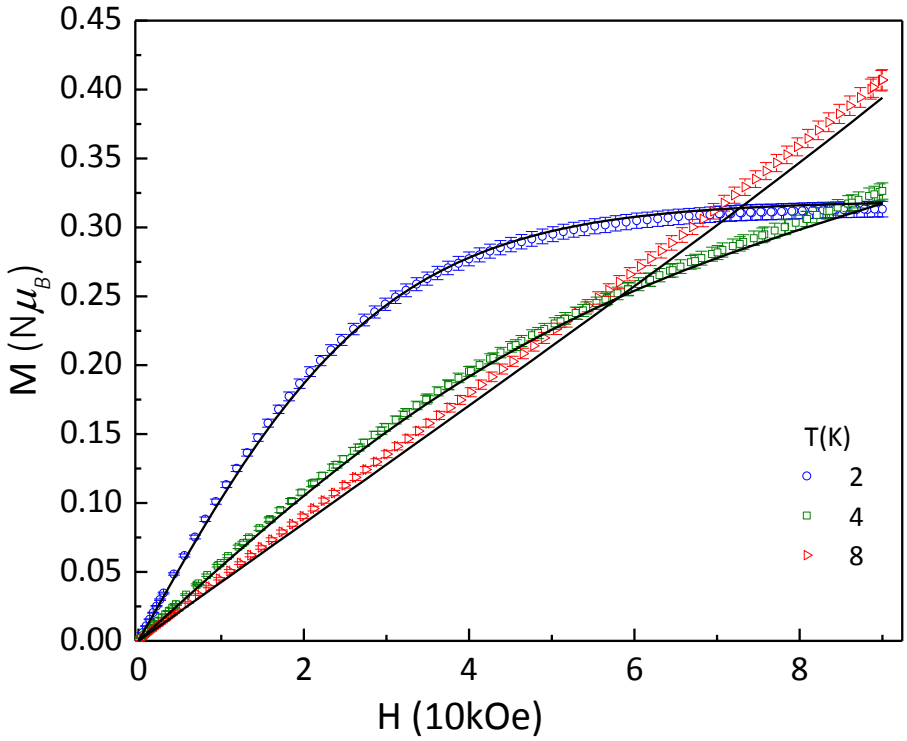

Fig. S9. : Field dependence of magnetization for **4** at different temperatures. Solid lines represent the best fits using parameters described in the main text.

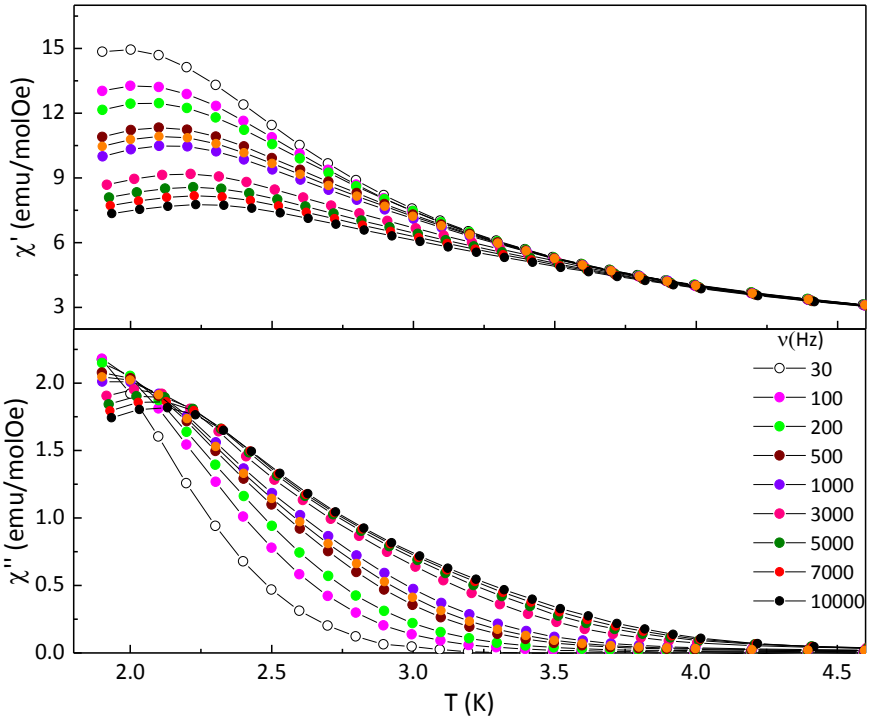

Fig. S10: Temperature dependence of real (χ´) and imaginary (χ´´) magnetic susceptibilities at different frequencies for **2** with solid lines as guide for eyes.

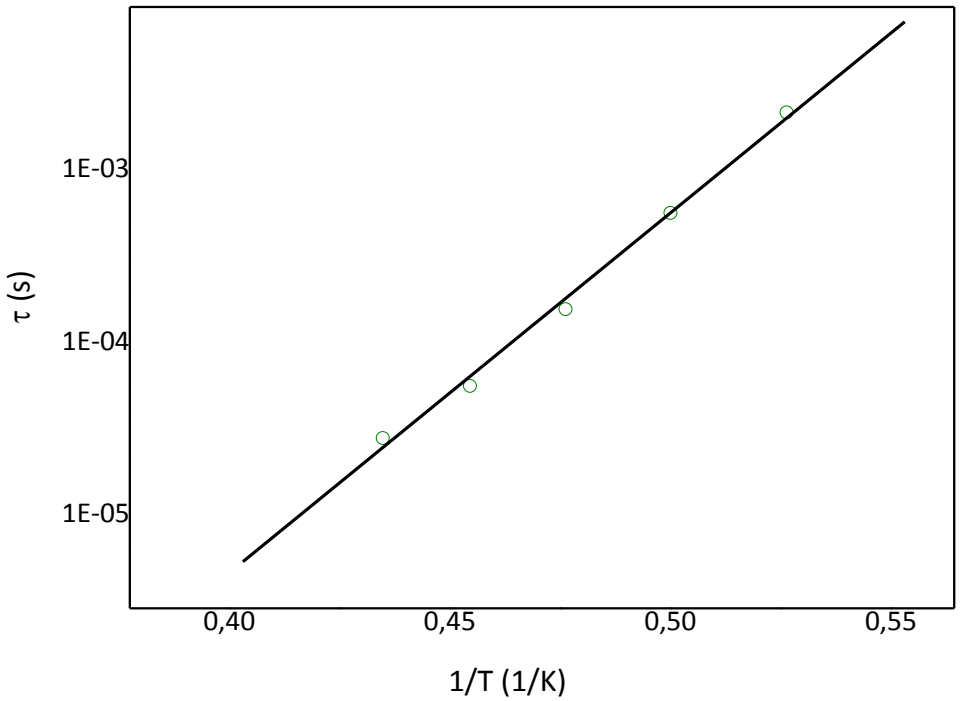

Fig. S11: Plot of τ as a function of the reciprocal temperature for **2**, where black line represents a fit using Arrhenius law.

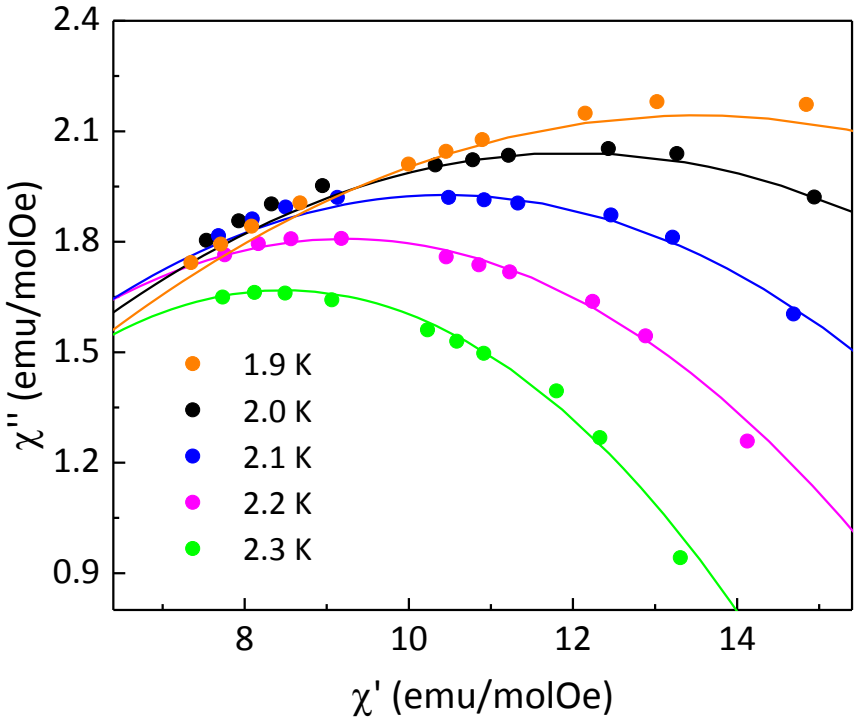

Fig. S12. The Argand plot for compound **2**, where the lines represent the best fit using a generalized Debye model.[1]

Table S4. Cole-Cole parameters obtained and used to reproduce the Argand plots.

Temperature (K)	χ_S (emu/K Oe)	χ_T (emu/K Oe)	α	τ (s)
1.9	5×10^{-10}	27.00	0.80	2.1×10^{-3}
2.0	2×10^{-6}	23.98	0.79	5.6×10^{-4}
2.1	3×10^{-14}	20.91	0.77	1.6×10^{-4}
2.2	1×10^{-3}	18.46	0.75	5.6×10^{-5}
2.3	0.9	16.03	0.72	2.8×10^{-5}

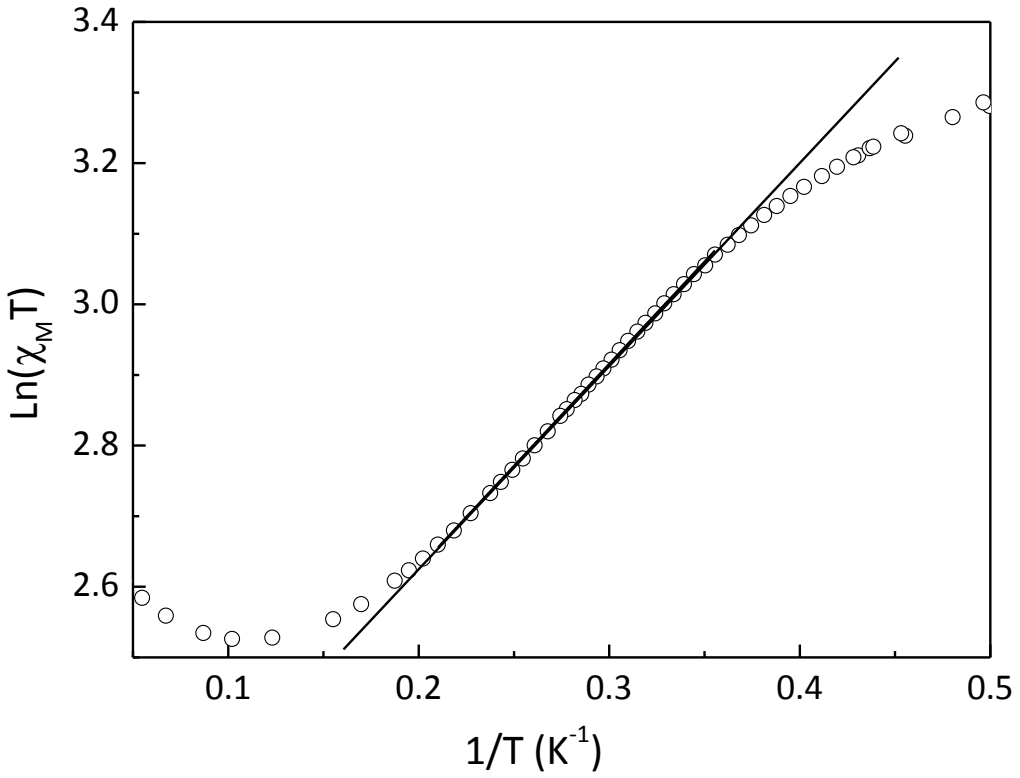

Fig. S13. : Plot of ln(χT) versus 1/T for **2** at 200 Oe dc field. Solid line corresponds to a linear fit according to an expression described in the main text.

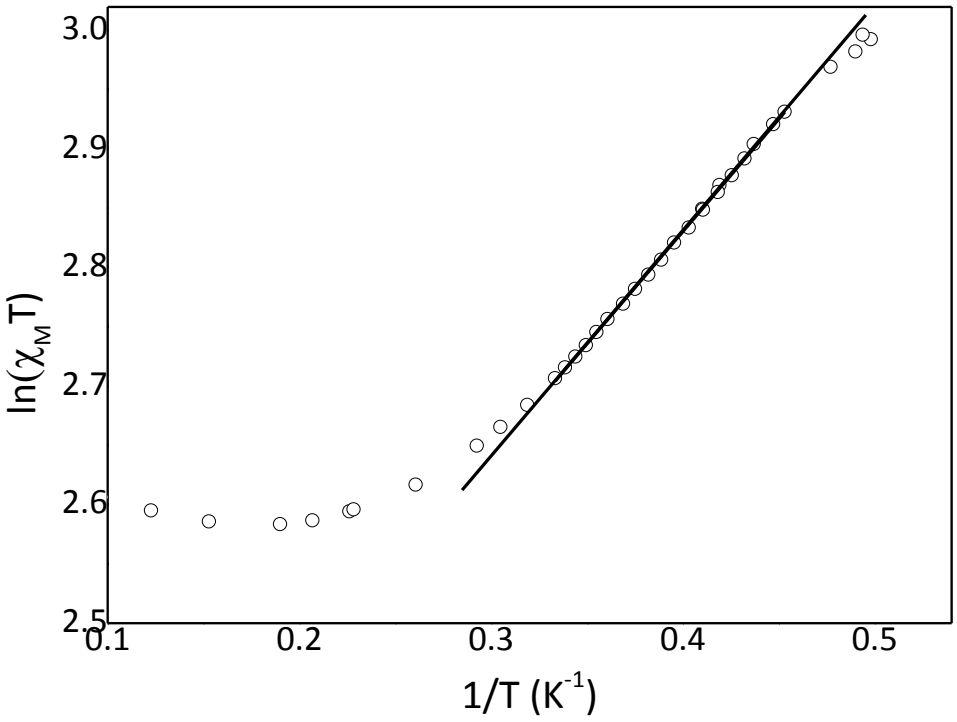

Fig. S14. : Plot of ln(χT) versus 1/T for **3** at 200 Oe dc field. Solid line corresponds to a linear fit according to an expression described in the main text.

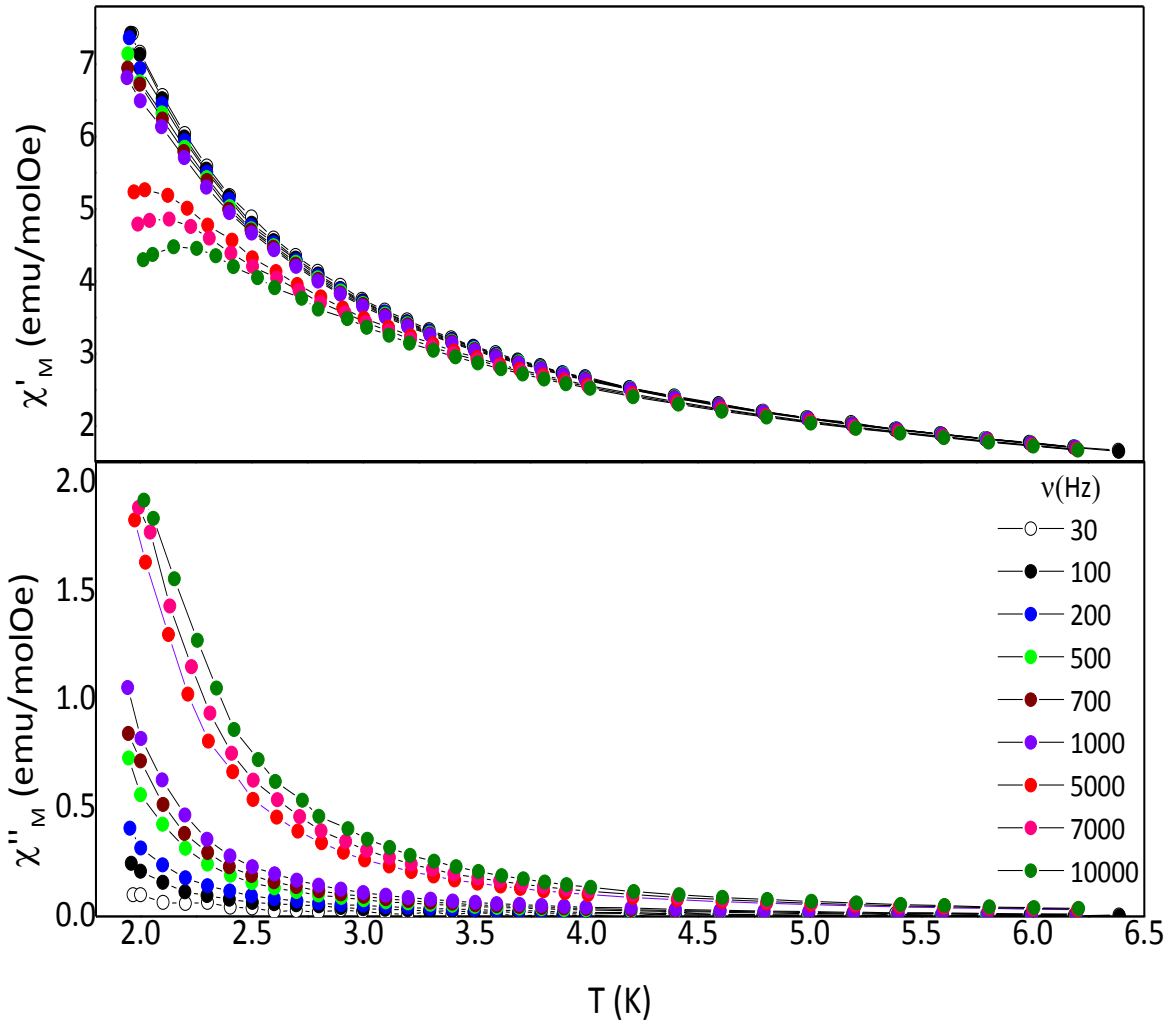

Fig. S15: Temperature dependence of χ´ and χ´´ at different frequencies at zero applied dc field for **3**. Solid lines are guide for eyes.

References

[1] K. S. Cole and R. H. Cole, *J. Chem. Phys.* 1941, **9**, 341-351.